

Optimization of the surface initiated polymerization of molecular imprinted methacrylate polymer on gold electrode for the detection of testosterone

A. Betatache^{a,b}, F. Lagarde^a and N. Jaffrezic-Renault^{a*}

^a *University of Lyon, Institute of Analytical sciences, 69100 Villeurbanne, France*

^b *University of Jijel, Jijel 18000, Algeria*

*Corresponding author. Email :Nicole.jaffrezic@univ-lyon1.fr

Received date: Jan. 01, 2018; revised date: Apr. 28, 2018; accepted date: May 03, 2018

Abstract

In this work a sensor based on molecularly imprinted polymer (MIP) was fabricated to detect testosterone which is an endocrine disruptor. The methacrylic MIP is polymerized on the gold electrode surface, through the grafting of the initiator 2,2'-Azobis(2-Amidinopropane) (APA) on gold surface. A mixed SAM was firstly built from 1-hexanethiol and an alkanethiol bearing carboxyl end groups whose chain length determines the distance of (APA) initiator from the surface of the gold electrode. Ferrocene-carboxylic acid was used to quantify free amine group of the (APA) initiator fixed on mixed SAM without bridging and ferrocenyl methyl methacrylate was used to check through cyclic voltammetry (CV) that methacrylate monomers polymerize on the electrode surface. Using these tools, the SAM composition was optimized as 1-hexanethiol (HT): 11-mercaptoundecanoic acid (AMU) with a molar ration of 50/50. The detection of testosterone with the MIP-sensor was done using electrochemical impedance spectroscopy. A linear range of 1pg/L to 1 ng/L was obtained, with a detection limit of 1 pg/L.

Keywords: *sensor; molecularly imprinted polymer; testosterone; polymethacrylate; cyclic voltammetry; electrochemical impedancespectroscopy.*

1. Introduction

Accurate and sensitive determination of testosterone becomes an important requirement to meet physical examination and disease diagnosis. Until now, a wide range of analytical methods is available for testosterone detection in biological fluids, including HPLC, GC-MS and LC-MS. However, these methods do need expensive instruments, specialized personnel, and much time to get the results, which limit the routine use. Meanwhile, many immunological assays were developed founded on the recognition of antigens by antibodies in clinical diagnosis. Nevertheless, the immunoassays mentioned above are often laborious and time-consuming, and a major limiting factor is the large requirement of high-quality testosterone-specific antibodies, which have hindered their further wide applications. Electrochemical immunosensors with lower sample consumption, less cost of instrumentations, good sensitivity, and accurate and visible results as the main reasons, have been widely used in many marker detections. Electrochemical impedance spectroscopy (EIS) is useful for evaluating the interfacial properties of

biochemical and biophysical processes with high specificity and sensitivity. Information can be collected from the signal alteration influenced by the adsorbing of target analytes to the functionalized surface of the electrodes. EIS has been widely applied for immunosensors fabrication. Nevertheless, the use of antibody limits the shelf-life of the immunosensor. In this work a biomimetic sensor, based on MIP polymethacrylate is developed for the detection of testosterone. Molecularly imprinted polymers (MIPs) are crosslinked polymers with specific binding for a particular analyte [1,2]. These binding sites are tailor-made in situ by the copolymerization of functional and crosslinking monomers in the presence of a print molecule called "template". After polymerization, the removal of template leaves recognition sites that are complementary to the print molecule in terms of size, shape and functionality [3]. Then, ideally, a molecular memory is introduced in the polymer by the imprinting process, which results in selective rebinding of the template in preference to other closely related molecules [4,5]. Methacrylic acid was used like functional monomer, ethylene glycol dimethacrylate as crosslinking monomer and acetonitrile as porogen solvent.

The immobilization of the MIP layer on the surface of the electrochemical transducer is an important aspect for the realization of an integrated sensor. The contact between the MIP layer and the transducer must be as perfect as possible to minimize parasitic effects of the environment and the dropout of the MIP layer. In principle, the ultrathin polymer films can be obtained by *in situ* polymerization techniques such as polymerization initiated from the surface [6,7], electropolymerization on an electrode [8,9], spin-coating of monomers followed by a photopolymerization [10] or spin-coating of polymer solutions containing the preformed imprint molecule "template". In the *in situ* polymerization method, the covalent bond may be accomplished either by the "grafting to" approach or by the "grafting from" approach. In the "grafting to" approach, the surface of the solid substrate is functionalized with polymerizable monomers, the initiator is in solution with monomers and the polymerization is initiated in solution, the monomers attached to the surface of the solid substrate polymerize with monomers from the solution and thus a thin film is formed on the surface of the solid substrate but the disadvantage with this approach is the low density of the polymer at the surface of the substrate and the inhomogeneity of the polymer film. The "grafting from" is the most promising approach in the synthesis of the polymer brushes with high graft density; the initiator is first immobilized on the surface of the solid substrate. It allows the obtaining of a thin film polymer attached to the surface [11]. An alternative is the use of the self-assembly technique for fixing a grafting a monolayer on the surface of the transducer before anchoring the initiator.

In this work we used the "grafting from" approach for the manufacturing of a sensor based on molecularly imprinted polymers (MIPs) polymethacrylate for testosterone detection. The azoic initiator, 2,2'-Azobis(2-amidinopropane) (APA), was fixed on a mixed self-assembled monolayer of alkanethiols previously fixed on the gold electrode surface. The different steps of functionalized electrodes (SAM formation, initiator (APA) immobilization and MIP polymerization on gold electrode) were characterized using cyclic voltammetry (CV). We have also shown the testosterone detection capabilities by the MIP-sensor obtained in this work through electrochemical impedance spectroscopy (EIS).

2. Experimental section

2.1. Origin of the reagents

1-hexanethiol (HT 95%), thioglycolic acid (ATG, 80%), 6-mercaptohexanoic acid (AMH 90%), 11-mercaptoundecanoic acid (AMU, 95%), N-hydroxysuccinimide (NHS, 98%), ethylene glycol dimethacrylate (EGDMA, 99%), methacrylic acid (MA, 99%), N-(3-dimethylaminopropyl)-N'-ethylenecarbodiimide hydrochloride (EDC), testosterone (T, >99%), 2,2'-Azobis(2-amidinopropane) (APA, 97%), ferrocenylmethyl methacrylate (FMMA, 95%), ferrocene-carboxylic acid (97%), N,N-dimethylformamide (DMF, 99.8%), methanol (99.8%), ethanol (99.8%), tetrahydrofuran (THF, 99.9%), $K_3Fe(CN)_6$ (>99%), $K_4Fe(CN)_6 \cdot 3H_2O$ and tablets for the preparation of alkaline phosphate buffer saline (pH=7.5) were purchased from Sigma-Aldrich and used as received. All aqueous solutions were prepared using ultrapure water (resistivity 18.2M Ω .cm) obtained using a Millipore purification system.

2.2. Preparation of gold electrodes:

The gold substrates were provided by the laboratory for Analysis and Architecture of systems (LAAS, CNRS Toulouse). They were manufactured using standard silicon technologies. Oriented Silicon wafers of (100) P-type (3-5 Ω .cm) were thermally oxidized to grow an oxide layer of 800 nm thick followed by a gold layer of 300 nm thickness deposited by vacuum evaporation. A 30 nm-thick titanium underlayer allowed for a better adhesion of gold on the silica surface. The wafer was cut into 1 \times 1 cm² square plates. Before use the gold electrode were washed with acetone for 15 min in an ultrasonic bath, dried with nitrogen, and then cleaned using a fresh mixture H₂O₂:H₂SO₄ 3:7 v:v (Piranha) for 5 min rinsed with copious amounts of distilled water and ethanol and finally dried with nitrogen.

2.3. Formation of SAM and grafting of APA

Gold electrodes were immersed in ethanol solutions containing a total concentration of 3 mM of 1-hexanethiol (HT) et 11-mercaptoundecanoic acid (AMU) with different molar ratios of HT:AMU (0 :100, 25 :75, 50 :50, 75 :25, 100 :0). Two others electrodes were incubated in ethanol solutions degassed with nitrogen (N₂) with total concentration of 3 mM in a molar ratio of 50:50 of HT:ATG et HT:AMH. All electrodes were rinsed with absolute ethanol to remove the excess thiol and dried with N₂.

Gold electrodes functionalized with different molar ratio of mixed SAM of HT:AMU were incubated in solutions containing 20 mM of EDC and 20 mM of NHS in ultrapure water to activate carboxylic groups of thiol acid at the surface. After this step of activation, electrodes containing the activate carboxylic groups were incubated in dark in solution of ultrapure water

containing the azoic initiator (APA) with a molar concentration of 200 mM.

2.4. Photopolymerization of MIP polymethacrylate

First a gold electrode was functionalized with a mixed SAM of HT:AMU in a molar ratio of 50:50 and with the initiator APA. After the gold electrode functionalized with mixed SAM HT:AMU and the initiator (APA) was placed in a pre-polymerization solution prepared by dissolving 0.035 mole of methacrylic acid (MA), 0.0112 mol of ethylene glycoldimethacrylate (EGDMA) and 0.0014 mol of testosterone in 3.5 ml of acetonitrile. Before polymerization, the pre-polymerization solution was degazed with nitrogen N_2 for 15 min. All was placed in a photochemical reactor and irradiate under a UV lamp for 2 h ($\lambda = 365$ nm). Thus, the printed film of polymer grafted on the gold electrode was prepared. The MIP-sensor was washed with methanol for 2 hours to remove testosterone.

2.5. Electrochemical measurements

The impedance measurements were performed using a conventional three electrode system, the working electrode was the modified gold electrode (active surface area defined by an O-ring seal: 0.07 cm²), the counter electrode was the platinum electrode (active surface area defined by an O-ring seal: 0.21 cm²) and the reference electrode was an Ag/AgCl electrode. The measurements impedance were performed using Voltalab 80 (PGZ 402). The impedance analyses were performed with an ac voltage of 10 mV in a frequency range of 100 mHz to 100 kHz with applying a dc potential of +200 mV to minimize impedance of the interface. All electrochemical measurements were carried out at room temperature in a Faraday cage.

Cyclic voltammetry measurements were performed at a scanning rate of 100 mV.s⁻¹, at ambient temperature, in PBS solutions (pH=7.5) or in PBS solutions containing 5 mM of ferri/ferrocyanide.

3. Results and discussion

3.1. Study of the influence of the composition of the SAM layer on the initiator grafting

3.1.1. Effect of the chain length of acid alkanethiol

In figure 1, we observe that the oxydoreduction peaks of the ferri/ferrocyanide redox couple disappear

after the formation of the mixed SAM and reappear after grafting of the azoic initiator (APA). This phenomenon may be due to the bridging of the initiator as is shown in figure 2.

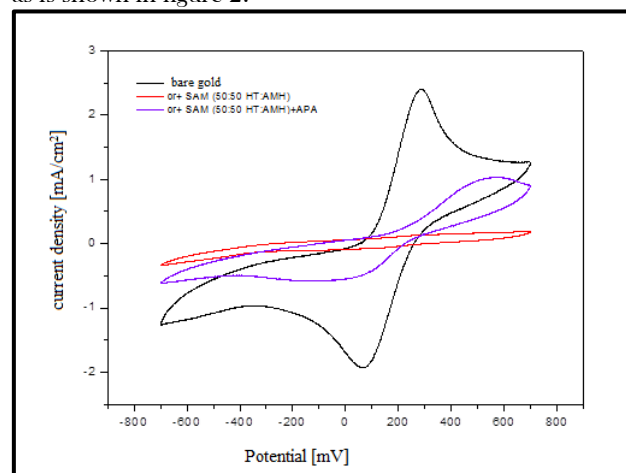


Figure1: Cyclic voltammograms for the characterization of mixed SAM (HT:AMH in the molar ratio of 50:50) before and after the grafting of the initiator. The scanning rate 100 mV.s⁻¹ in solution PBS pH=7.5, containing 5 mM of ferri/ferrocyanure.

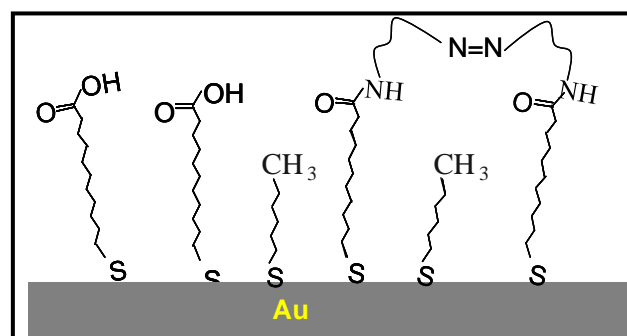


Figure 2: Proposed mechanism of the grafting of the initiator (APA) on the mixed SAM (HT:AMH at molar ratio of 50:50).

The bridging of the initiator could lead to the formation of holes in the mixed SAM and a higher exchange rate through the mixed SAM. This phenomenon could take place when the initiator grafting density is high enough. The effect of chain length of the acid alkanethiol on the bridging of the azoic initiator (APA), was determined by reporting the relative difference between the oxidation peak maximum on bare gold electrode and the oxidation peak maximum after the immobilization of the initiator (APA), versus the chain length of the acid alkanethiol, as shown in figure 3. It is observed that the smallest difference is obtained for $n=10$. The 11-mercaptoundecanoic acid was chosen for further studies.

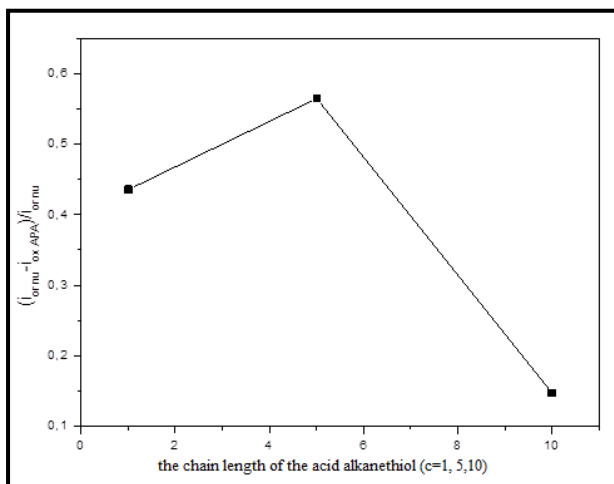


Figure 3: Relative difference between the oxidation peak maximum on bare gold electrode and the oxidation peak maximum after the fixation of the initiator (APA), versus the chain length of the acid alkanethiol (molar ratio 50:50).

3.1.2. Effect of the molar ratio of HT:AMU

To determine the optimal conditions for bridging of the initiator (APA), it was reported the relative difference between the oxidation peak maximum of the redox probe on bare electrode and the oxidation peak maximum after the immobilization of the initiator (APA) versus the molar ratio of mixed SAM (HT:AMU), as shown in Figure 4. The smaller value is obtained with the mixed SAM HT:AMU with the molar ratio of 50:50.

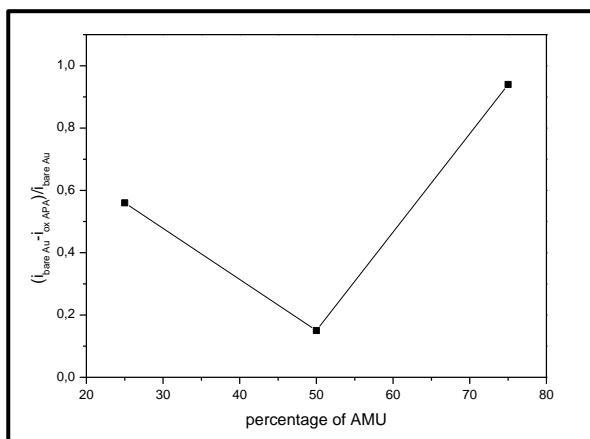


Figure 4: Relative difference between the oxidation peak maximum on bare gold electrode and the oxidation peak maximum after the fixation of the initiator (APA), versus the molar ratio of mixed SAM (HT:AMU)

3.1.3. Quantification of the free amine group (NH₂) of the azo-initiator (APA) versus molar ratio of the mixed SAM (HT:AMU)

The free amine group of the initiator is due to the lack of bridging of the azoic initiator. Gold electrodes functionalized with different molar ratio of mixed SAM HT:AMU (25:75, 50:50, 75:25) grafted with the initiator APA were incubated in a solution of DMF 2.5 ml containing 200 mM of EDC, 200 mM of NHS and 200 mM of FeCOOH to attach FeCOOH on the free amine groups (NH₂) of the initiator. Electrodes were then characterized using cyclic voltammetry in PBS solution pH=7.5, with scanning rate of 100 mV.s⁻¹ to observe the response of ferrocene.

In figure 5, we see the response of ferrocene attached to the mixed SAM HT:AMU 25:75 and we report the intensity of the redox peak maximum versus molar ratio of the mixed SAM HT:AMU, as shown in Figure 7. The highest response of the ferrocene is with the molar ratio 25:75 and the smallest one is with the molar ratio 75:25. We can conclude from these results that the bridging of the initiator (APA) is optimal with the molar ratio 50:50 of the mixed SAM HT:AMU.

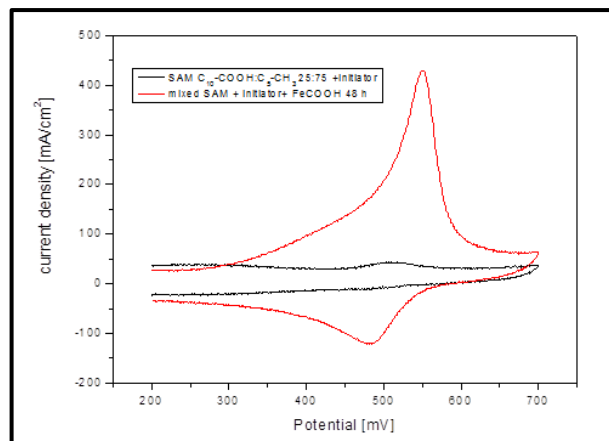


Figure 6: Cyclic voltammograms of mixed SAM HT:AMU (molar ratio 25:75) + initiator (APA) in PBS before and after the fixation of ferrocene carboxylic acid.

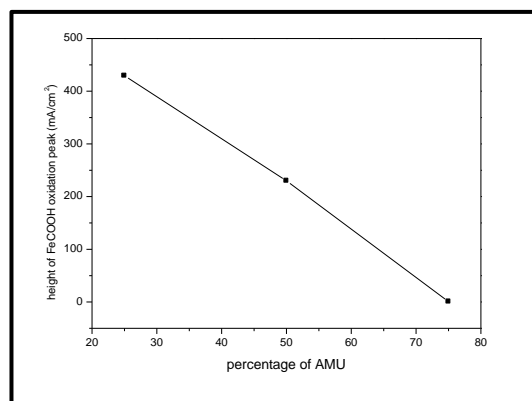


Figure 7: Intensity of the oxidation peak maximum of ferrocene carboxylic acid versus the molar ratio of the mixed SAM HT:AMU

3.2. Study of the influence of the composition of the SAM layer on the methylmethacrylate ferrocene polymerization

To determine in which molar ratio of the mixed SAM HT:AMU the best polymerization of methacrylate occurs, a methacrylate monomer containing ferrocene, the methylmethacrylate ferrocene (FMMA) was chosen to be polymerized on the top of the gold electrodes functionalized with mixed SAM and grafted initiator (APA). For this, a solution containing $5 \cdot 10^{-2}$ M of FMMA in THF was prepared. Gold electrodes functionalized with different molar ratio of mixed SAM HT:AMU (0:100, 25:75, 50:50, 75:25, 100:0) and grafted initiator (APA) were put in FMMA THF solution. All were introduced into a UV apparatus ($\lambda = 365$ nm) and irradiated for 2 h. Then the electrodes were rinsed with THF, then placed for 30 s under ultrasonication and dried under a N_2 flow. Electrodes were then characterized using cyclic voltammetry in PBS solution pH=7.5, with a scan rate of $100 \text{ mV}\cdot\text{s}^{-1}$ to observe the response of ferrocene.

In figure 8, we observe that redox probe ferrocene, contained in FMMA, is well and truly present in the polymerized layer on gold electrode: redox peaks of ferrocene at 518 mV and 457 mV.

In figure 9, it appears that the intensity of the oxidation peak maximum of the probe ferrocene is greater in the molar ratio 50:50 of the mixed SAM HT:AMU, so at this molar ratio, polymerization occurs on the surface of the electrodes, in agreement with the higher bridging density of the initiator.

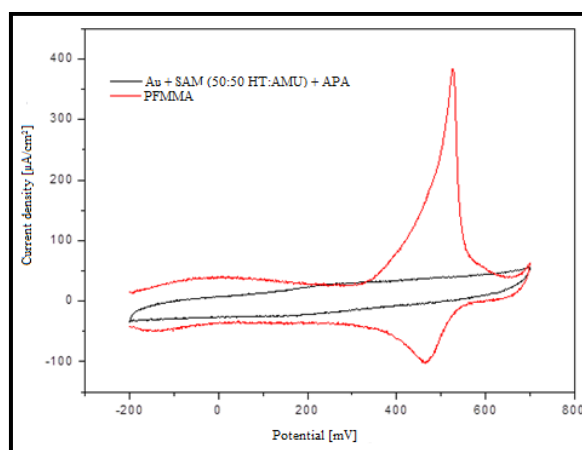


Figure 8: Cyclic voltammograms of the mixed SAM HT:AMU in the molar ratio 50:50 before and after polymerization of FMMA. Scanning rate $100 \text{ mV}\cdot\text{s}^{-1}$ in a solution of PBS at pH=7.5.

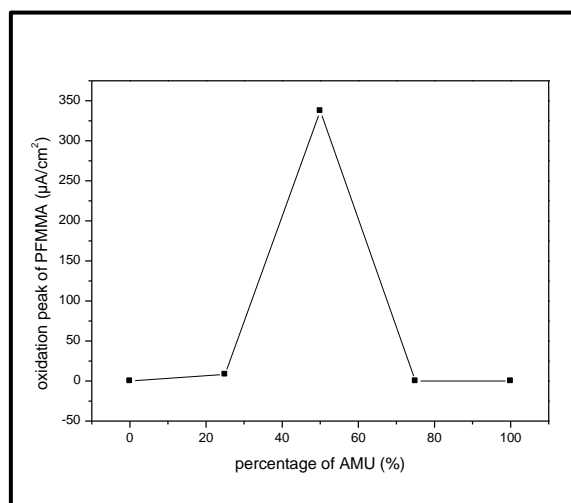


Figure 9: Variation of the intensity of the oxidation peak maximum of ferrocene in PFMMA polymerized on gold electrode versus molar ratio of mixed SAM HT:AMU

3.3. Analytical performance of the MIP based sensor for testosterone detection.

The testosterone MIP film of polymethacrylate was deposited on the functionalized gold electrode, as described in §2.4. The MIP film was washed with methanol for 2 hrs for removing testosterone template. The MIP base sensor was put in the three-electrode cell, filled with a PBS solution containing 5 mM of ferro/ferricyanide, with different concentrations of testosterone.

In figure 10, we observe that impedance increases with the increase of the concentration of testosterone between $1 \text{ pg}\cdot\text{l}^{-1}$ et $1 \text{ ng}\cdot\text{l}^{-1}$. This is due to the neutral charge of testosterone, by completing the printed sites in the MIP film, it decreases the charge transfer through the film. Beyond the concentration of $1 \text{ ng}\cdot\text{l}^{-1}$, there is no variation of impedance, this being due to the saturation of printed sites in the MIP film.

The electrical behavior of the MIP-sensor/electrolyte interface can be modeled according to the Randle electrical circuit presented in figure 11. Using this circuit, the impedance spectra have been modeled with the software Zview. Then the relative variation of the charge transfer resistance (R_{tc}) is plotted versus the concentration of testosterone in figure 12. In this latter figure, the calibration curve for testosterone is linear between $1 \text{ pg}\cdot\text{l}^{-1}$ and $1 \text{ ng}\cdot\text{l}^{-1}$, with a sensitivity of $0.28/\text{ng}\cdot\text{l}^{-1}$ and a detection limit of $1 \text{ pg}\cdot\text{l}^{-1}$. This detection limit is very low, compared to that of the impedimetric immunosensor recently developed ($45 \text{ ng}\cdot\text{l}^{-1}$) [12]. The NIP film was also tested for the detection of testosterone, compared to MIP film, the NIP film has a

very low sensitivity for testosterone (sensitivity: 0.048/ng.l⁻¹). The sensor has been washed and reused four times in a week, it was reproducible with relative standard deviation ranging between 4% for 4 different sensors and 16% for the reuse of the same sensor.

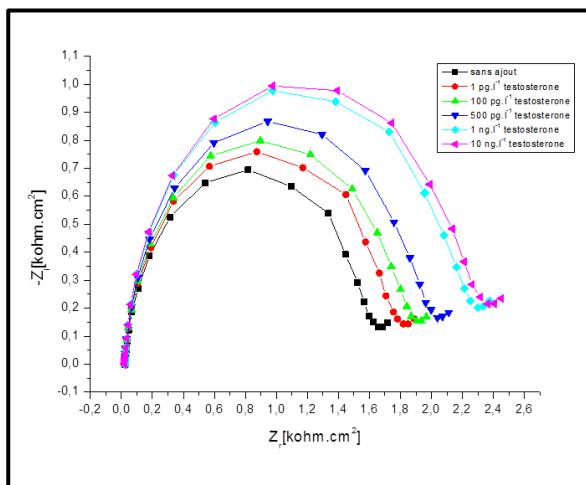


Figure 10: Nyquist impedance spectra of the MIP based sensor in different concentrations of testosterone. Measurements of EIS were performed in a solution of PBS containing 5 mM of ferri/ferrocyanide.

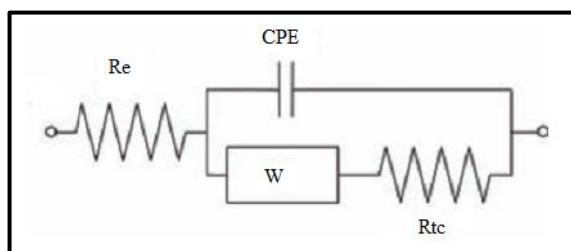


Figure 11: Diagram of an equivalent electrical circuit of an electrode with faradaic reaction and diffusional control (Randles circuit) .

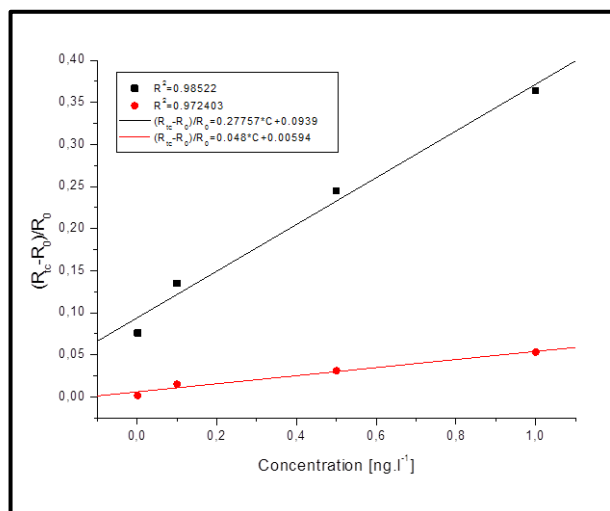


Figure 12: Calibration curves of MIP and NIP based sensors versus testosterone concentration. All measurements were carried out in a PBS solution at pH=7.5, containing 5 mM of Ferri/Ferrocyanide.

4. Conclusion

After the optimization of the SAM composition for a higher bridging density of the azoic initiator, the capabilities of the MIP-sensor to detect testosterone were evaluated. The sensor detects in a linear range of 1 pg.l⁻¹ to 1 ng.l⁻¹ with a detection limit of 1 pg.l⁻¹. A NIP-sensor was also fabricated and tested for the detection of testosterone, the sensitivity toward testosterone was only 17% of that of the MIP-sensor. The advantage of the photopolymerization used in the case of polymetacrylates is that it allows localized polymerization and can be used for the realization of MIP based multi-sensor to detect different targets.

Acknowledgement: The authors thank French and Algerian government for PROFAS grant.

References

- [1] G.M. Murray, G.E. Southard, in: M. Yan, G. Ramstrom (Eds.), Marcel Dekker, New York (2005) 579.
- [2] B. Sellergren, F. Lanza, Molecularly Imprinted Polymers, Elsevier, New York, (2001) ISBN: 9780444828378
- [3] T. Prasada Rao, R. Kala, An overview Talanta, 76 (2008) 485.
- [4] E. Yilmaz, K. Haupt, K. Mosbach, Angew. Chem. Int. Ed. 39 (2000) 2115.
- [5] S.C. Zimmerman, N.G. Lemcoff, Chem. Comm. (2004) 5.
- [6] T. Piacham, A. Josell, H. Arwin, V. Prachayasittikul, L. Ye, Anal. Chem. Acta., 536 (2005) 191.
- [7] X. Wei, X. Li, S. M. Husson, 6 (2005) 1113.
- [8] B. S. Ebarvia, S. Cabanilla, F. Sevilla, 66 (2005), 145.
- [9] A. Gómez-Caballero, M. Aranzazu Goicolea, Ramón J. Barrio, Analyst, 130 (2005) 1012.
- [10] R.H. Schmidt, K. Mosbach, K. Haupt, Advanced Materials, 16 (2004) 719.
- [11] M. Hussenman, E. E. Malmstrom, M. Mc Namara, M. Mate, M. Mecerreyes, D. G. Benoit, J. L. Hedrick, P. Mansky, E. Huang, T. P. Russell, C. J. Hawker, Macromolecules, 32 (1999) 1424.
- [12] G. Li, M. Zhu, L. Ma, J. Yang, X. Lu, Y. Shen, Y. Wan, ACS Appl. Mater. Interf. 8 (2016) 13830